A CMOS Wireless Two-axis Digital Accelerometer Using Bondwire Inertial Sensing

Y.-T. Liao, J. Shi, and B. Otis
Electrical Engineering Department, University of Washington, Seattle, USA

ABSTRACT
This paper presents a two-axis wireless accelerometer using bondwire inertial sensing without MEMS processing. The bondwire sensors are bonded chip-to-chip to reduce the manufacturing uncertainty. The accelerometer consists of oscillator-based inductance-to-frequency converters, a digital frequency demodulator, and a 400 MHz FSK wireless transmitter. A digitally programmable interface allows the digitalization of acceleration information and control of bandwidth and resolution of the sensor system. The accelerometer has a transducer gain of 7.5 kHz/g and a bandwidth of 1.2 kHz while consuming 63 mW.

KEYWORDS
Inertial sensor, accelerometer, oscillator, bondwire, wireless transmitter, inductance sensitivity

I. INTRODUCTION
Accelerometers have wide application in consumer electronics and medical applications for orientation/tilt detection and patient activity monitoring. The physical transduction mechanisms underlying MEMS accelerometers [1] provide stable and accurate acceleration detection. However, the fabrication cost is relatively high due to the complicated process compared to standard IC fabrication.

Our previous work demonstrated an accelerometer using a bondwire inertial sensor in a standard CMOS process and a plastic lead chip carrier package without MEMS processing [2]. A dense and relatively elastic gold (Au) wire is used in conjunction with a less dense and stiff aluminum (Al) wire. The difference in material properties creates a relative deflection between the two bondwires during acceleration, causing a mutual impedance change that can be detected using on-chip electronics.

In a sensor system, wired connections usually limit the mobility and flexibility of sensors and may cause detection errors. Integrating sensor, signal processing, and wireless radio on a single chip can significantly reduce fabrication cost, improve sensor performance, and enhance range of operation.

In this paper, we present a single chip wireless two-axis digital accelerometer. The bondwire sensors are bonded chip-to-chip to solve the following limitations of acceleration gain variations due to manufacture deviation and detection errors from package/board stress and wire connections [3].

II. BONDWIRE MODEL
Bondwires are typically 1-5 mm long, have a 26 μm (1mil) diameter, are composed of gold or aluminum, and trace an approximately parabolic arc. Under acceleration, bondwires exhibit mechanical detection that is especially prominent at the apex of the parabolic curve. The peak displacement per acceleration of gravity (g) at the apex of a semicircular bondwire is derived as [4]

$$\frac{\Delta X}{g} = \frac{\rho R^4}{Er^2}(2\pi + \pi^2) \quad (1)$$

where R is the radius of the semicircle, r is the radius of the wire, E is the Young's modulus, and ρ is the density. From equation (1), changing a bondwire's geometry or material properties will result in a change in the magnitude of the wire's deflection for a given acceleration. Bondwire electrical properties depend on their physical dimensions--the height above the die plane, the horizontal length, and the distance between adjacent bondwires. For two bondwires of equal length, the mutual inductance is approximately

$$M \approx \frac{\mu_o l}{2\pi}\left[\ln\left(\frac{2l}{D}\right) - 1 + \frac{D}{l}\right] \quad (2)$$

where l is the length of the bondwires and D is the distance between them. The inductive sensitivity increases with the length due to the increased mutual inductance contribution in total inductance. When the length is much larger than the separation between two bondwires, the mutual inductance becomes logarithmically dependent on the length of bondwires.

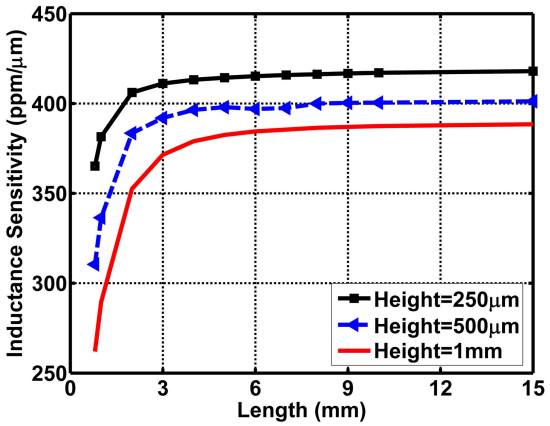

Fig. 1 FEM simulated results of inductive sensitivity (separation between two bondwires = 90 um)

Fig. 1 shows the finite element method (FEM) simulated result of inductance sensitivity/displacement. The separation between two bondwires is 90 μm, which is the minimum on-chip bonding pad separation. To miniaturize the sensor size without sacrificing sensitivity, 3 mm bondwires are chosen, which have an inductive sensitivity of 390 ppm/μm.

III. READOUT CIRCUITRY DESIGN
To detect the small inductance changes, we proposed FM readout architecture. Fig. 2 shows the system block

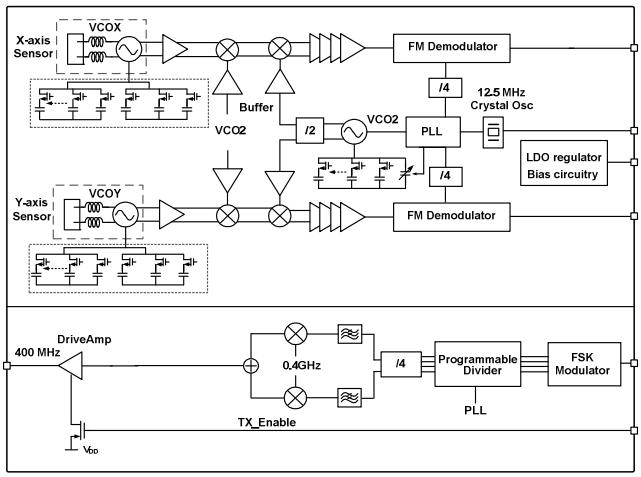

Fig. 2 Block diagram of the IC

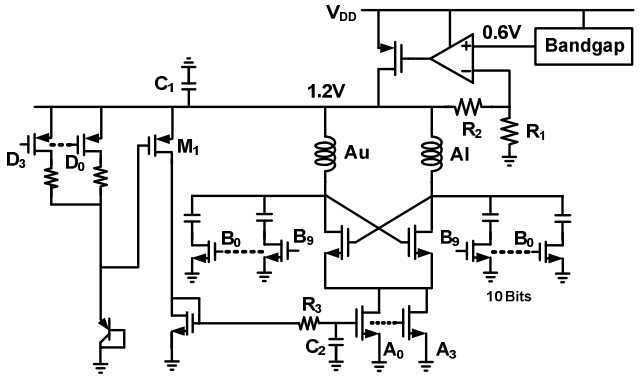

Fig. 3 Schematic of bondwire sensing oscillator

diagram of the wireless accelerometer. The architecture includes two identical acceleration sensor readout circuits (for 2-axis sensing), a digital frequency demodulator, and a 400 MHz wireless transmitter. Readout circuits consist of a 2.4 GHz oscillator that senses mutual inductance variation caused by acceleration and converts inductance changes into a frequency-modulated RF signal. Fully-differential downconversion architecture provides common mode noise suppression. A low noise on-chip, low drop-out (LDO) regulator and bandgap reference are employed to reduce supply pushing and provide stable voltage supply.

To facilitate accurate detection of small frequency shifts and to avoid oscillator pulling and injection locking, Two-step downconversion architecture is used to translate the frequency from 2.4 GHz to 2 MHz. A phase locked loop (PLL) generates a stable 1.6GHz frequency reference. 800MHz and 400MHz quadrature clock signals for the digital controller, modulator, and transmitter are divided from PLL outputs using current mode logic (CML) and static logic dividers.

After downconversion, a counter-based frequency demodulator (FDM) digitizes the baseband signal to 36 bits. The counting windows can be adjusted to different lengths, leading to effective control of the resolution and bandwidth. The decoded signals, stored in a 320-bit buffer, can be observed in parallel or in series outputs

A 400MHz Medical Implant Communication Service (MICS) band transmitter was designed for on-body

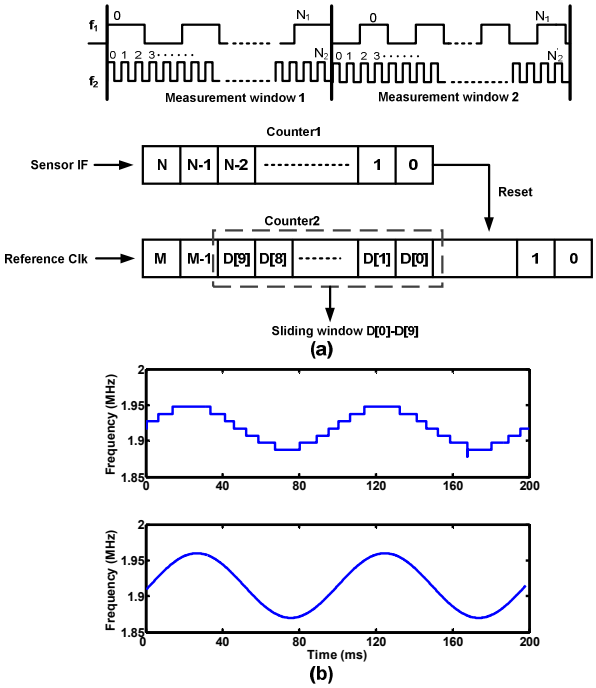

Fig. 4 Operation of frequency demodulator and measured digitalization result of a sinusoidal input

medical applications. To save power, the transmitter is activated in a short duty cycle only when the on-chip buffer is full.

A. Bondwire sensing oscillator design

Oscillator phase noise (short term uncertainty) and frequency drift (long term uncertainty) are indistinguishable from acceleration-induced frequency shifts. Thus, the goal of the sensing oscillator design was to reduce phase noise and frequency drifts caused by the power supply and temperature variations. Fig. 3 shows the proposed architecture of the bondwire oscillator.

To reduce supply pushing, a low drop out regulator provides a temperature-stable, power supply-independent 1.2 V output to the oscillator. The regulator achieves measured power supply rejection ratio (PSRR) of 30 dB and a voltage drift less than 10 mV over the temperature range of 20-100 ^{o}C.

A PTAT temperature sensor using a BJT and resistors is placed close to the oscillator to track temperature-related biasing changes of the oscillator. A frequency compensation scheme [5] is used to reduce temperature-caused frequency drifts by a feedback of temperature sensor current to control the oscillator. The slope of feedback bias current can be controlled by the 3-bit trimming resistors (D0-D3) and 4-bit switching current mirrors (A0-A3). The temperature-compensated oscillator achieves a 500ppm frequency variation, comparing to 3000ppm in the uncompensated oscillator in the temperature range of 20-60 ^{o}C.

B. Reconfigurable digital frequency demodulator

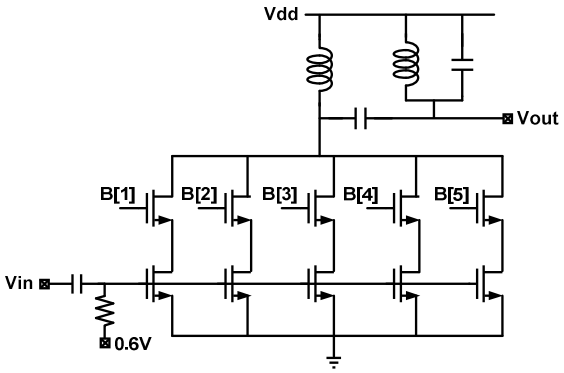

Fig.5 Schematic of driver amplifier

A digital FM demodulator was designed to convert the IF signal to digital output of the demodulated signal. The core logic for the frequency calculation uses two variable-length counters that implement a frequency counting algorithm shown in Fig 4(a). The N bit counter clocked by the sensor IF signal counts up until a reconfigurable limit N_1 is reached and determines the duration of the measurement window. The M bit counter clocked by the PLL clock (CLK) counts the total number of CLK periods N_2 in the measurement window. The variation of the sensing IF signal can be calculated as:

$$\Delta f_{IF} = N_1 f_{ref} \frac{\Delta N_2}{(N_2 + \Delta N_2) \cdot N_2} \approx \frac{N_1 f_{ref}}{N_2^2} \cdot \Delta N_2 \qquad (3)$$

The resolution of the digital FM demodulator, namely the minimum detectable frequency variation, is $N_1 \cdot f_{ref}/N_2^2$, which can be improved by using a higher frequency reference clock or increasing the length of the measuring window. However, the bandwidth (B) of the acceleration signal places a restriction on the maximum duration of the measurement window. According to Nyquist sampling theorem, to accurately demodulate the acceleration signal, $N_1 < f_{IF}/2B$. The window length can be reconfigured on-the-fly by using the on-chip digital controller to meet different measurement bandwidth and resolution requirements. To save bandwidth during transmission, a programmable sliding window is applied to the 36-bit counter to transmit a 10-bit differential frequency measurement. The higher stable bits are transmitted only once at the beginning of the measurement. Other transmission bits represent the frequency deviations of sensing information. Fig. 4(b) shows the input IF frequency converted from measurement results with a 10Hz sinusoidal frequency modulation signal input at 1.9MHz.

C. Wireless transmitter

A 400 MHz FSK transmitter was implemented with a direct modulation method using open-loop divider architecture. A 100 MHz baseband signal is first divided by the programmable modulation divider and then mixed with the carrier frequency. In FSK mode, two sets of divider ratios are generated according to the transmission data values.

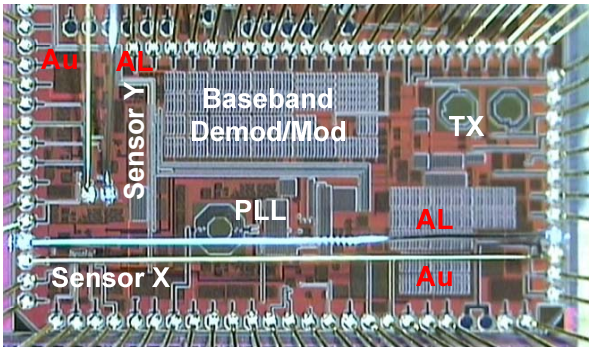

Fig. 6 Micrograph of the bondwire accelerometer

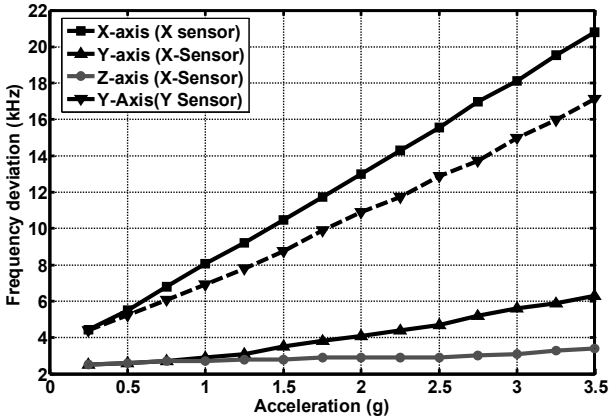

Fig. 7 Measured 3-axis of acceleration

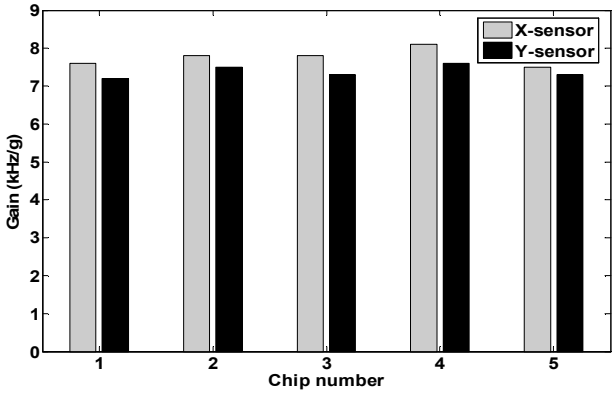

Fig. 8 Measured transducer gain of 5 chips

Digital I/Q outputs from the FSK modulator must be shaped to minimize the inter-symbol interference and limit signal bandwidth. A third order RC low-pass filter is used to attenuate the harmonic terms above the cut-off frequency, 1 MHz.

The 400 MHz transmitter is implemented using direct upconversion. The quadrature LO signals (400 MHz) are generated by dividing from the PLL output (1.6 GHz). The data transmission using FSK modulation is realized by hopping from two dividing ratios in the programmable divider.

Fig. 5 shows the driving amplifier, which uses a cascode structure to assure isolation from the PA driver output to its input and to maintain the stability of the driver amplifier. The output power of the PA driver is controlled by switching the cascode transistors on or off. A power control range of 12dB is achieved by 4 steps of

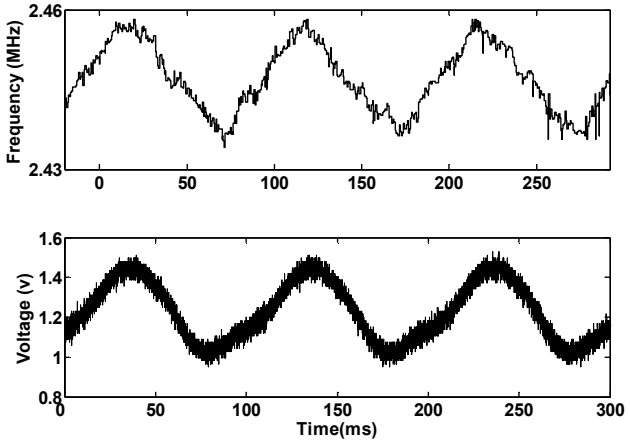

Fig. 9 Measured results of waveform at 10 Hz sinusoidal acceleration input with a 3g peak-to-peak amplitude (x-axis)

3dB each. An on-chip matching network converts the high output impedance of driver amplifier to a 50Ω. The driving amplifier achieves maximum output power of -16dBm and provides a 12 dB linear gain control through switching parallel amplifiers.

IV. MEASUREMENT RESULTS

The wireless accelerometer was implemented using a 0.13μm CMOS process (Fig. 6). The sensors and TX are placed on the opposite sides of the chip to reduce pulling when the TX is turned on. The design is fully integrated in an area of 3.2 x1.85 mm^2. Two bondwire sensors are placed orthogonally to allow two-axis sensing. To enhance the precision of bonding and eliminate board/package stress, the sensing bondwires are bonded chip-to-chip (instead of chip-to-package), to achieve better control of the length and separation of the wires.

The accelerometer was assembled on a printed board and mounted to a custom machined aluminum platform to maximize the mechanical energy transferred from a shaker table to the accelerometer.

Fig. 7 shows the measurement results of a 3-axis acceleration test on the bondwire accelerometer, revealing a linear gain of 7.5 kHz/g and 6.9 kHz/g in sensitive X-axis and Y-axis, respectively. 15dB isolation between the sensitive and non-sensitive axes is demonstrated. The X-and Y-sensors exhibit a 0.6 kHz/g gain deviations among 5 chips (Fig. 8), likely due to bonding process/strength variation and device mismatching. The bandwidth of our bondwire accelerometer is 1.2 kHz, limited by the mechanical resonance frequency of the gold bondwire. The measurement resolution can be controlled by the digital frequency demodulator. Fig. 9 shows the measured waveform of a 10 Hz sinusoidal acceleration signal with a 3g peak-to-peak acceleration applied to the chip, along with an on-board commercial accelerometer. Each sinusoidal cycle contains 244 measurement samples. The frequency output (upper) was decoded from the measured digital codes, and the analog output (bottom) was the result of the reference accelerometer. Digital outputs are

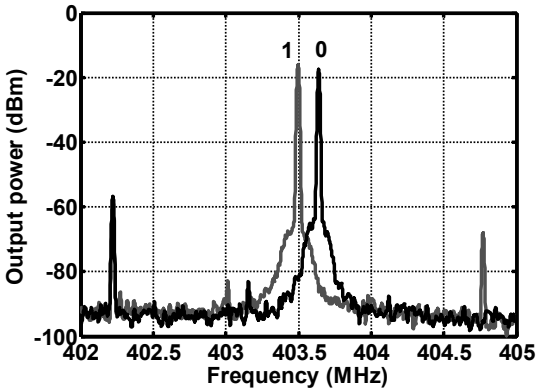

Fig. 10 Measured FSK transmitter output spectrum

less susceptible to power supply noise and interference. Fig. 10 shows the measured transmitter output spectrum. The frequency deviation between data "0" and "1" is 150 kHz.

V. CONCLUSION

This paper presents a two-axis wireless digital accelerometer using bondwire inertial sensing. The accelerometer has a transducer gain of 7.5 kHz/g and 6.9 kHz/g in X-axis and Y-axis, respectively, a bandwidth of 1.2 kHz and a minimum detectable acceleration is 140 mg while consuming 63 mW. Without expensive and complicated MEMS processes and sensor integration, our design provides a low-cost single-chip solution for a wireless accelerometer. By exploiting standard IC technology, the proposed bondwire accelerometer provides reconfigurable bandwidth and resolution and is suitable for tilt/orientation detection in low cost consumer electronics and healthcare system.

VI. REFERENCE

[1] M. Paavola, M. Kamarainen, J. Jarvinen, M. Saukoski, M. Laiho, and K. Halonen, "A micropower interface ASIC for a capacitive 3-axis micro-accelerometer," *IEEE J. Solid-State Circuits*, vol. 42, no. 12, pp. 2651–2665, Dec. 2007.

[2] Y.-T. Liao, W. Biederman, and B. Otis, "A fully integrated CMOS accelerometer using bondwire inertial sensing," *IEEE Sensors Journal,* vol.11, no.1, pp.114-122, Jan. 2011.

[3] J. Craninckx, M. Steyaert, "A 1.8-GHz CMOS low-phase-noise voltage controlled oscillator with prescaler," *IEEE J. Solid-State Circuits,* vol.30, no.12, pp.1474-1482, Dec 1995.

[4] T. Marinis and J. Soucy, "Design and characterization of wirebonds for use in high shock environments," in Electronic Components and Technology Conference, pp. 1414-1422, May 2009.

[5] T. Wu, U.-K. Moon, and K. Mayaram, " Dependence of LC VCO oscillation frequency on bias current," IEEE International Symposium on Circuits and Systems, May, 2006.